DOI: 10.6060/mhc245880d

Possibilities of Thermal Lens Spectrometry in the Analysis of *p*-Chlorophenoxy Substituted Lutetium Phthalocyanine

Vladislav R. Khabibullin, Elena A. Gorbunova, Tatiana V. Dubinina,[@] and Mikhail A. Proskurnin

Department of Chemistry, Lomonosov Moscow State University, 119991 Moscow, Russian Federation
[@]Corresponding author E-mail: dubinina.t.vid@gmail.com

Dedicated to the memory of Academician of the Russian Academy of Sciences Oskar Iosifovich Koifman and Professor Boris Dmitrievich Berezin

The work assessed the physicochemical changes in p-chlorophenoxy-substituted lutetium phthalocyanine in chloroform and tetrahydrofuran under the influence of laser radiation. For this purpose, thermal lens spectrometry was used, as combining optical molecular spectroscopy and thermophysical analysis. A significant change in the thermal diffusivity of the phthalocyanine was detected, which is probably a consequence of the specific solvation of phthalocyanine macromolecules at a level of 10 nmol/L. A change in the thermal lens signal over 12–16 h indicates photoinduced activity of the phthalocyanine.

Keywords: Phthalocyanine, thermal lens spectrometry, aggregation, photodegradation, UV-Vis spectroscopy.

Возможности термолинзовой спектрометрии в анализе *пара*-хлорфеноксизамещенного фталоцианината лютеция

В. Р. Хабибуллин, Е. А. Горбунова, Т. В. Дубинина,[@] М.А. Проскурнин

Химический факультет, Московский государственный университет имени М.В. Ломоносова, 119991 Москва, Российская Федерация
[@]E-mail: dubinina.t.vid@gmail.com

Посвящается памяти академика РАН Оскара Иосифовича Койфмана и профессора Бориса Дмитриевича Берёзина

В работе проводилась оценка протекающих под действием лазерного излучения физико-химических изменений пара-хлорфеноксизамещенного фталоцианината лютеция в хлороформе и тетрагидрофуране. Для этого применялась термолинзовая спектрометрия, которая совмещает молекулярную оптическую спектроскопию и теплофизический анализ. Обнаружено значительное изменение температуропроводности фталоцианина, что может быть следствием специфической сольватации макромолекул фталоцианина на уровне 10 нмоль/л. Изменение термолинзового сигнала в течение 12–16 часов указывает на фото-индуцируемую активность фталоцианина.

Ключевые слова: Фталоцианин, термолинзовая спектрометрия, агрегация, фотодеградация, электронная спектроскопия поглощения.

Introduction

Phthalocyanines and their tetrapyrrolic analogs are prospective compounds for organic electronics and medicinal chemistry. Phthalocyanines can be applied as photoactive layers in solar cells[1,2] and sensors,[3] in light-activated catalytic reactions,[4] photodynamic therapy,[5,6] and fluorescent imaging.[7-9] Unlike their analogues, porphyrins and chlorins, phthalocyanines have higher thermal and photochemical stability, constant chemical composition, as well as an intense absorption maximum at the boundary of the visible and near-IR regions. Porphyrins and chlorins have the most intense absorption maximum in the UV region compared to those in the visible and near-IR ranges,[10] while the opposite is characteristic of phthalocyanines.[11] Many applications of phthalocyanines involve the use of lasers: nonlinear optics, photodynamic therapy, and catalysis. Thus, studying the behavior of phthalocyanines and especially their stability during laser ionization is an important task.

Thermal lens spectrometry (TLS), a method of photothermal spectroscopy, is based on recording changes in the refractive index of a medium due to nonradiative relaxation of excited molecules.[12] This provides simultaneous analysis of the optical (light absorption, temperature gradient of the refractive index of the medium) and thermal parameters of the object (thermal diffusivity, thermal conductivity, and heat capacity) under high-power laser radiation in a broad wavelength range.[13-15] Wide capabilities of this method have found application in the analysis of biological objects, environmental science, chemical analysis, energy, and materials science.[14,16-23]

Simultaneous recording of several signals in TLS has found application in the quantitative and qualitative analysis of complex multicomponent systems, in which classical spectrophotometry is not always sufficient.[24,25] With the advent of heat-conducting nanofluids (dispersions of nano or microparticles), the need to measure heat capacity, thermal conductivity, and thermal diffusivity has increased, as evidenced by a large number of studies.[26-29]

TLS makes it possible to record changes in physicochemical properties of objects over time at low absorption and analyte concentrations.[30] A separate area of application of thermal lens spectrometry is the study of reaction kinetics, analysis of photochemical systems and objects exhibiting photoinduced activity.[17,18,31,32] The kinetics of transesterification and complex formation were studied.[31,33-35] In[36], photothermal analysis of aqueous dispersions of graphene oxide revealed the photoinduced decomposition of graphene oxide into individual clusters and partial reduction occurring under the action of laser radiation.

In this work, we studied the laser-based effects on the thermal diffusivity of *p*-chlorophenoxy substituted lutetium phthalocyanine in chloroform and tetrahydrofuran using double-beam thermal lens spectrometry at low concentrations (10 nmol/L). TLS revealed photoinduced activity under the influence of laser radiation. Based on the results obtained, assumptions were made about the nature of the existence of phthalocyanine in solutions.

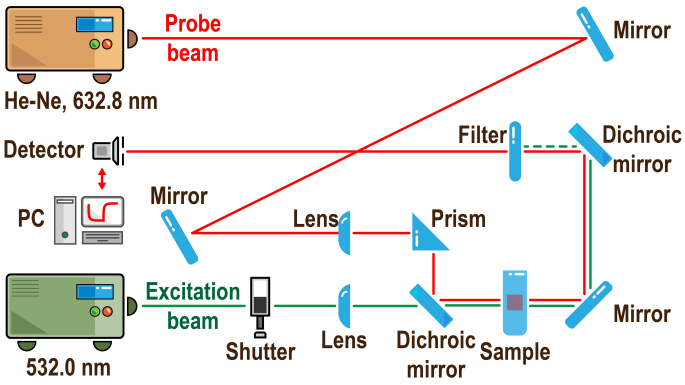

Figure 1. Schematic of a dual-beam thermal lens spectrometer.

Experimental

Photothermal measurements

Photothermal measurements were carried out on a double-beam thermal lens spectrometer (Figure 1). High-power solid-state laser radiation (λ_e = 532 nm, TEM_{00}) passes through a shutter, which is controlled by an analog-to-digital and digital-to-analog converter (ADC) connected to a personal computer (PC) and enters the sample in a quartz cell (l = 10.00 mm). In the sample, due to the absorption of laser energy and non-radiative relaxation, a temperature gradient arises acting as a scattering lens (a thermal lens). A low-power helium-neon laser (λ_p = 632.8 nm, TEM_{00}), which expands when passing through a thermal lens, was used as a probe laser. This leads to a drop in the initial intensity of the probe beam at the detector. A photodiode was used as a detector.

One measurement cycle begins when the shutter opens, continues when the shutter closes, and ends when the shutter opens again, after which the cycle repeats. The PC receives data from the ADC and detector, which are processed in the original program, where they are formed, displayed and stored in the form of transient curves of heating and dissipation of the thermal lens (signal intensity *vs*. time).

To describe the behavior of the probe laser on the detector, the Shen-Snook model for two-beam thermal lens spectrometry in a steady state was used, described in detail in [37]. The transition curve equation describing the intensity of the probe laser at the detector $I(t)$ depends on the initial intensity of the probe beam $I(0)$, geometric parameters m and V, thermo-optical signal θ and characteristic time t_c:

$$I(t) = I(0)\left[1 - \frac{\theta}{2}\tan^{-1}\left(\frac{2mV}{[(1+2m)^2+V^2](t_c/2t)+1+2m+V^2}\right)\right]^2 \quad (1)$$

If for m, V and θ all coefficients and constants are, as a rule, known in advance (measured or from reference data and optical measurements) and the parameters are found according to the equations specified in[37] then the characteristic time t_c is an experimental parameter that is associated with thermal diffusivity (D) according to the following equation:

$$t_c = \omega_{e0}^2/4D, \quad (2)$$

where ω_{e0} is the radius of the inducing beam in the sample.

The stationary thermal lens signal is found using the following equation:

$$\theta = \frac{I(0) - I(\infty)}{I(0)} \quad (3)$$

where $I(\infty)$ is the intensity of the probe beam in a steady state, with the thermal lens fully developed. The operating principle, determination of thermal diffusivity and thermal lens signal by the TLS method for complex systems are described in detail.[36,38] The operating parameters of the measurements are given in the *Supplementary materials,* Table S1.

General

Electronic absorption (UV-Vis) spectra were recorded on a JASCO V-770 spectrophotometer using quartz cells (1×1 cm). High-resolution matrix assisted laser desorption/ionization time-of-flight (MALDI-TOF/TOF) mass spectra were taken on a Bruker Autoflex II mass spectrometer with α-cyano-4-hydroxy-cinnamic acid (CHCA) as the matrix. ^{1}H NMR spectra were recorded on a Bruker AVANCE 600 spectrometer (600.13 MHz). Chemical shifts are given in ppm relative to $SiMe_4$. Attenuated Total Reflection-Fourier Transform Infrared spectroscopy (ATR-FTIR) was carried out using a Thermo Scientific Nicolet iS5 FT-IR spectrometer; spectral resolution, 4 cm^{-1}.

Synthesis

Method A. Approach with 4,5-(p-chlorophenoxy)phthalonitrile

*Octa(p-chlorophenoxy)substituted phthalocyanine lutetium(III) acetate **4***. A mixture of phthalonitrile **1** (100.00 mg, 0.26 mmol), $Lu(OAc)_3{\times}4H_2O$ (55.00 mg, 0.13 mmol) and 1,8-diazabicyclo(5.4.0)undec-7-ene (DBU) (39 μL, 0.26 mmol) was refluxed in isoamyl alcohol (2 mL) with stirring for 4 h (TLC-control: SiO_2, F_{254},toluene). The reaction mixture was cooled to room temperature and MeOH:H_2O (4:1, V:V) was added. The precipitate was filtered and washed with MeOH:H_2O (4:1, V:V). This yielded 122.00 mg (54%) of compound **4**. UV-Vis (THF) λ_{max} nm (lgε): 356 (4.94), 609 (4.53), 675 (5.39). IR (diamond) ν cm^{-1}: 1010–1089 (st C–Cl); 1373–1398 (γ pyrrol); 1267–1282 (st Ph-O), 1373–1484 (st COO^- sym); 1531–1583 (st COO^- as); 2331–2362 (residual CO_2). MS (MALDI-TOF) *m/z*: 1695 [M-OAc]$^+$. MS (MALDI-TOF/TOF) *m/z*: 1694.9857 [M-OAc]$^+$. Calculated for $C_{80}H_{40}Cl_8LuN_8O_8$: 1694.9885 [M-OAc]$^+$. ^{1}H NMR (600 MHz, THF-d_8) δ_H ppm: 7.11–7.39 (m, 32H, H_{Ar}), 9.10 (s, 8H H_{Pc}).

Method B. Approach via octa(p-chlorophenoxy)substituted phthalocyanine

*Octa(p-chlorophenoxy)substituted magnesium phthalocyanine **2***. A mixture of phthalonitrile **1** (200.00 mg, 0.53 mmol), $Mg(OAc)_2{\times}4H_2O$ (28.50 mg, 0.133 mmol) and DBU (20 μL, 0.133 mmol) was refluxed in isoamyl alcohol (2 mL) with stirring for 4 h (TLC-control: SiO_2, F_{254},toluene). The reaction mixture was cooled to room temperature and MeOH:H_2O (4:1, V:V) was added. The precipitate was filtered and washed with MeOH:H_2O (4:1, V:V). This yielded 199.00 mg (97%) of compound **2**. UV-Vis (THF) λ_{max} nm (lgε): 358 (4.71), 607 (4.32), 673 (5.10). MS (MALDI-TOF/TOF) *m/z*: 1545 [M+H]$^+$. MS (MALDI-TOF/TOF) *m/z*: 1545.0428 [M+H]$^+$. Calculated for $C_{80}H_{40}Cl_8MgN_8O_8$: 1545.0400 [M+H]$^+$. ^{1}H NMR (600 MHz, THF-d_8) δ_H ppm: 7.16–7.40 (m, 32H, H_{Ar}), 9.10 (s, 8H H_{Pc}).

*Octa(p-chlorophenoxy)substituted phthalocyanine **3***. Magnesium complex **2** (100.0 mg, 0.065 mol) was dissolved in concentrated sulfuric acid (10 mL), kept in an ultrasonic bath for 1-2 min. The resulting solution was poured on ice. The resulting green precipitate was filtered and washed with water (to a neutral pH), and then MeOH. This yielded 74.00 mg (75%) of compound **3**. UV–Vis (THF) λ_{max} nm (lgε): 348 (4.78), 664 (5.00), 698 (5.04). MS (MALDI-TOF/TOF): *m/z* 1525 [M]$^+$. MS (MALDI-TOF/TOF): *m/z* Found: 1525.8541 [M]$^+$. Calculated for $C_{32}H_{10}Cl_8N_8$: 1525.8534 [M]$^+$. ^{1}H NMR (600 MHz, THF-d_8) δ_H ppm: 7.58–7.90 (m, 32H, H_{Ar}), 10.26 (s, 8H H_{Pc}).

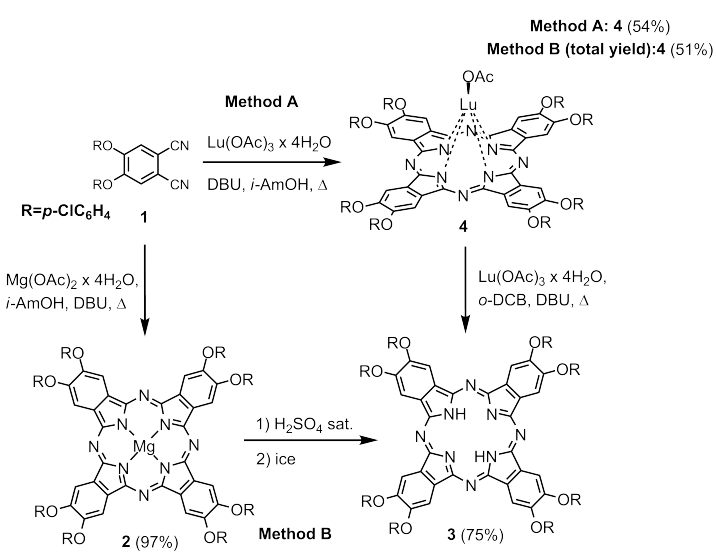

Scheme 1.

*Octa(p-chlorophenoxy)substituted phthalocyanine lutetium(III) acetate **4***. A mixture of ligand **3** (100.0 mg, 0.066 mmol), $Lu(OAc)_3{\times}4H_2O$ (55.0 mg, 0.132 mmol) and DBU (7 μL, 0.046 mmol) was refluxed in *o*-dichlorobenzene (*o*-DHB) (2 mL) for 4 h (TLC-control: SiO_2, F_{254},toluene). The reaction mass was cooled to room temperature and MeOH:H_2O (4:1, V:V) was planted. The precipitate was filtered and washed with MeOH:H_2O (4:1, V:V). This yielded 81.0 mg (70%) of complex **4**. The characteristics were identical with those obtained by *Method A*.

Results and Discussion

p-Chlorophenoxy substituted lutetium phthalocyanine **4** was prepared by two methods: a template method starting from a dinitrile and a multi-stage approach to phthalocyanine ligand including metalation (Scheme 1). The template method was slightly more effective for complex **4**. In order to avoid the formation of a by-product of the sandwich structure, lutetium acetate was taken in excess both with respect to the nitrile (Method A) and with respect to the phthalocyanine ligand (Method B).

All the compounds obtained were identified using high resolution mass spectrometry. Figure S1 shows the mass spectrum of the lutetium complex measured in the positive ion mode. There is one peak that can be assigned to the cleavage of axial acetate during laser ionization. High-resolution spectra of complexes demonstrate good agreement between the observed and calculated masses. Additionally, calculated and experimentally obtained isotopic pattern coincides well.

To prove the presence of axial acetate in the synthesized monophthalocyanine complexes, IR spectra were measured. As an example, Figure S3 shows the IR spectrum of target complex. Stretching vibrations of C–Cl bonds were observed in the range of 1089–1010 cm^{-1}. Vibrations corresponding to aryloxy fragments were observed in the range of 1282–1267 cm^{-1}. Skeletal vibrations of pyrrole fragments were detected in the region of 1398–1373 cm^{-1}. Bands at 1583–1531 and 1384–1373 cm^{-1} were assigned to carboxylate antisymmetric and symmetric stretching vibrations, respectively. Also, in the region of 2362–2331 cm^{-1}, residual CO_2 vibrations were observed.

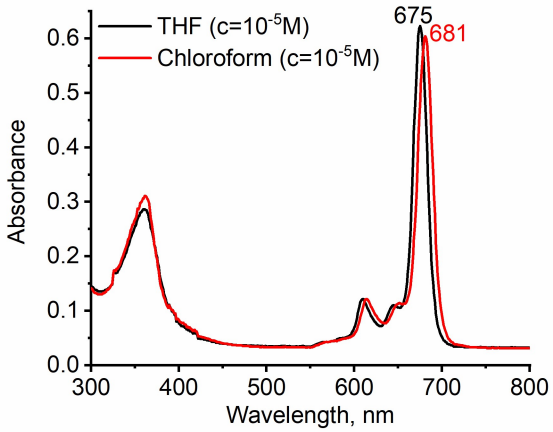

Figure 2. UV–Vis spectra of lutetium complex **4**.

UV–Vis spectrum of the lutetium complex **4** is presented in Figure 2. Two main absorption bands were observed which are typical for phthalocyanine complexes:[39,40] the most intense Q band in visible region and a Soret band in the UV region. Both B and Q bands originate from the π→π* transition and belong to the molecular orbitals of the phthalocyanine macrocycle. In addition, two Q band satellites were observed at wavelengths of 600–650 nm. Chloroform and THF were selected as solvents, in which the target complex shows good solubility. When using chloroform instead of THF as a solvent, a bathochromic shift of the Q band was observed. The concentration dependences of absorption for complex **4** obey Beer's law in the concentration range up to $2.5 \cdot 10^{-5}$ M (Figure S4). The logε values for the Q band are 5.42 and 5.39 for chloroform and THF solutions, respectively.

Despite the fact that the optical properties of phthalocyanines are very commonly presented in the literature,[41-44] examples of studying their properties using thermal lens spectroscopy have not been described. For thermal lens spectrometry, the issue of the correctness of photothermal measurements occupies an important place. To confirm the correct operation of the spectrometer and measurement conditions, as a rule, measurements of the thermal diffusivity of a pure solvent (ethanol, toluene, acetonitrile, water, *etc*.) are carried out. In our case, measurements were carried out for chloroform and THF. Figure 3 shows transient curves for chloroform and THF on linear and logarithmic scales.

In the analysis of thermal characteristics, the most informative part of the transient curves is the first 100–150 ms, in the range of which the thermal diffusivity is found. In this range, any deviations from the model transition curve have a physical meaning and indicate side thermal effects in the system (convection, thermophoresis) caused by physicochemical, optical, and/or morphological changes.[45,46] As noted previously,[38] the form of representation of transient curves on a logarithmic scale (Figure 3,b) allows one to distinguish thermal effects with a bias of less than 0.01%.

It was found that the experimental transient curves correlate well with the model (Figure 3), which indicates the absence of accompanying thermal and optical effects. The found average (n = 3) thermal diffusivities for chloroform and THF were 0.089, 0.091 and 0.115 mm^2/s, respectively, which is in good agreement with reference data.[47] The relative standard deviation in all cases did not exceed 2%. Thus, the thermal lens spectrometer operates under the optimum measurement parameters.

Next, photothermal measurements of *p*-chlorophenoxy substituted lutetium phthalocyanine with a concentration of 10 nmol/L were carried out in chloroform and THF. The dynamics of the development of transient curves for solutions of phthalocyanine in chloroform and THF have similar shapes. Figure 4 shows normalized transient curves for a solution in chloroform. In all cases, slow heating of the irradiated zone is observed. The thermal diffusivity found for the phthalocyanine in chloroform and tetrahydrofuran was 0.040 and 0.069 mm^2/s, respectively, which is 40–50% lower than the values for pure solvents.

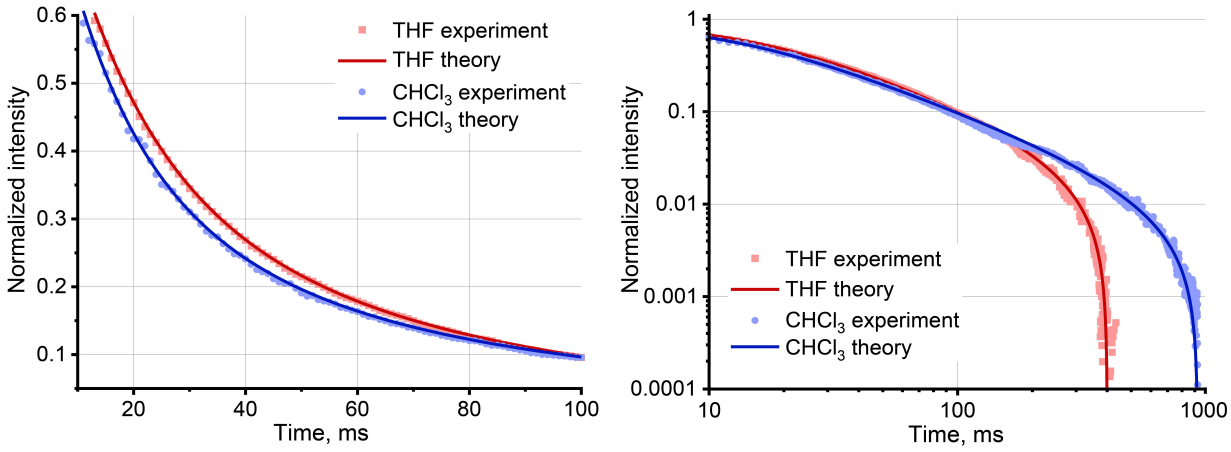

Figure 3. Experimental and theoretical transient thermal-lens heating curves for chloroform and THF in (a) linear and (b) logarithmic coordinates (laser power, 62 mW).

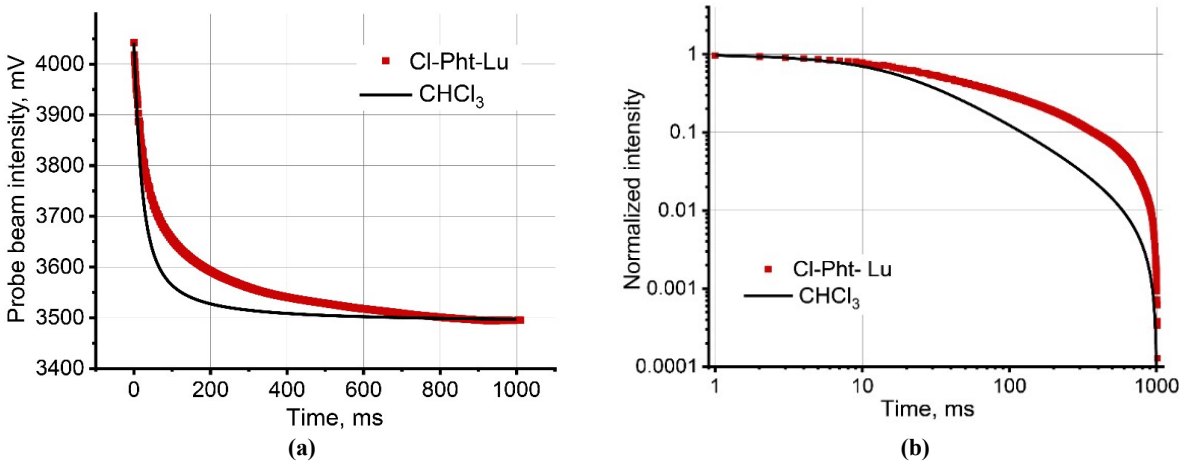

Figure 4. Transient thermal-lens heating curves for complex **4** in chloroform (10 nmol/L, laser power, 62 mW) in linear (a) and normalized logarithmic coordinates (b).

This effect on thermal parameters is typical for heterogeneous solutions.[29,48] In most cases, under the influence of laser radiation, the nanophase overheats and accelerates the heat transfer in solution, which increases obtained thermal diffusivity.[27,49] In this case, positive thermophoresis (the Soret effect) and thermal diffusion are observed, which manifest themselves as a larger intensity of the probe beam after 100–300 ms of development of the transient curve.[50,51] Less commonly, the presence of a nanophase reduces thermal diffusivity. In this case, the dispersed phase accumulates heat and slowly dissipates it. Previously, such behavior was discovered for an aqueous dispersion of graphene oxide.[36] With increasing concentration, the thermal diffusivity passed through a minimum value, which was 0.036 mm^2/s.

Transient dissipation curves for solutions of *p*-chlorophenoxy substituted lutetium phthalocyanine **4** in chloroform and tetrahydrofuran also have similar behavior. For solutions, slower cooling is observed than for pure solvents. Figure 5 shows transient dissipation curves for complex **4** in chloroform and pure chloroform.

The observed behavior is not typical for true solutions. On the other hand, such dynamics of transient curves is not typical for systems with photoinduced activity. As a rule, for such systems thermal diffusion is observed, which manifests itself in the transient curves after 100 ms of irradiation as an increase in intensity. The shape of the transient curve in this case has an extremum at 50–100 ms, with a subsequent increase in the intensity of the probe beam and reaching an equilibrium value, which is not observed in our case.[18,32,52]

The dynamics of the development of the thermal field are significantly influenced not only by the processes of aggregation/disaggregation that are observed in heterogeneous systems,[28,53,54] but also by structure-forming and structure-destructive effects caused by the components of the solution.[55] The content of substances in micro- and large quantities can lead to changes in the solution properties (changes in mass diffusion, density, thermal diffusivity, *etc*.).[56] This has been repeatedly shown for aqueous-organic solutions[57-59] and solutions containing surfactants,[60-62] salts,[63-65] polymer compounds,[51,66,67] *etc*. Photothermal studies have shown that the main causes of the observed effects are solvation (polarization of molecules, changes in the temperature refractive index of the medium, changes in the expansion coefficient).[51,64,68] It is known that phthalocyanines in small quantities significantly affect the optical properties of the medium.[12] This may be due to the fact that phthalocyanines can change the structure of the solvent, which manifests itself at distances comparable to the size of the formed structures. Previously,[69] it was established that the degree of influence of a component on the structure of the solvent also depends on the nature of the solvent. The content of Tartrazine dye above 10^{-7} mol/L and Rhodamine 6G above 10^{-6} mol/L also led to a change in the thermal properties of the solution.[70,71] The distance between Tartrazine molecules at a concentration of 10^{-7} mol/L[70] ($d_{av} \approx 0.735c^{-1/3}$) is *ca.* 160 nm, with a molecule volume of 5 nm^3.[72] In our case, for 10^{-8} mol/L *p*-chlorophenoxy substituted lutetium phthalocyanine, the average distance between the molecules was *ca.* 340 nm. In this case, the volume of a phthalocyanine molecule, according to [73] is about 10 nm^3. A comparison of the results using the size:distance ratio showed similar values: for Tartrazine and phthalocyanine 1:32 and 1:34, respectively, indicating a possibly similar nature of the influence of substances on the solvent.

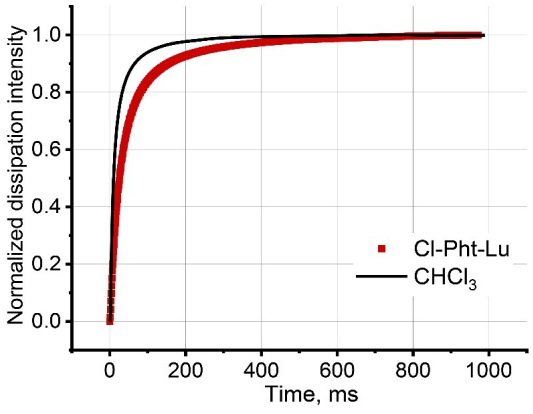

Figure 5. Normalized transient thermal-lens dissipation curves for complex **4** in chloroform (10 nmol/L, laser power, 62 mW).

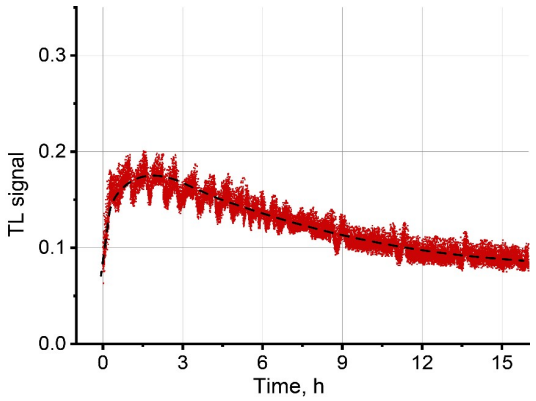

Figure 6. Thermal lens signal of *p*-chlorophenoxy substituted lutetium phthalocyanine in chloroform (10 nmol/L, laser power, 62 mW).

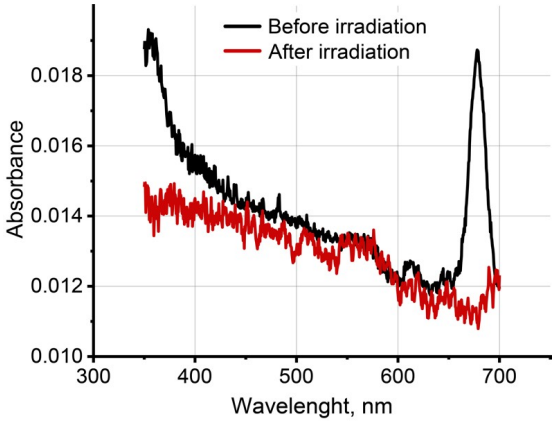

Figure 7. Optical spectra of *p*-chlorophenoxy substituted lutetium phthalocyanine in chloroform (10 nmol/L).

Thus, the observed thermal effects in a complex **4** solution may be associated with significant solvation of the molecule, which leads to a change in the structure of the solvent and, hence, a change in the physicochemical properties of the system.[74,75] Particular specific solvation contributes to the formation of ordered structures in solution: in a number of cases, the tendency of phthalocyanines to complex formation[76] and self-association,[77] was observed; spontaneous dimerization and aggregation were recorded. Sulfonic phthalocyanines of cobalt(II) exhibit structuring properties in the solvent.[78] But to study this phenomenon completely, additional experiments are required that are beyond the scope of this work.

Figure 6 shows a change in the photothermal signal over 16 h. In this case, complex dynamics of changes in the thermal lens signal is observed, which can be divided into two stages. During the first 1.5 h, a significant increase in the signal is observed, after which the signal slowly decreases, and after 12 h reaches a constant value corresponding to the initial state. This behavior is characteristic of a chemical reaction, where a change in the concentration of components leads to a change in absorption, which affects the thermal lens signal.[34,36]

In our case, *p*-chlorophenoxy substituted lutetium phthalocyanine demonstrates photoinduced activity. An initial increase in the signal indicates an increase in the number of absorbing particles and, thus, in the rate of the photoinduced reaction. Previously, this behavior was observed in[79], where, as a result of the reaction of potassium persulfate with potassium iodide, iodine was released, which absorbs the radiation of the excitation laser and enhances the power of the thermal lens. Over time, the release of iodine stopped, and the thermal lens signal reached an equilibrium value.[79]

Next, the concentration of the complex **4** in solution decreases. Previously, similar results were obtained in[52], where the authors observed a decrease in the thermal lens signal for the chromium 1,2-diphenylcarbazide complex (Cr-DPC) with every subsequent irradiation cycle. The authors explained this effect by a photochemical reaction occurring in the area of irradiation with the exciting beam, which decomposed Cr-DPC particles and led to a decrease in the concentration of absorbing particles.[52] At the same time, signal changes with a period of 40 min, which are observed already at the initial stage of analysis, may relate to the stabilization of the concentration gradient.[79] Here, the irradiation zone is periodically updated with unreacted phthalocyanine from the volume adjacent to the irradiated zone due to thermally induced convection.[12] This occurs until most of the original complex **4** reacts with radiation. Thus, phthalocyanine undergoes photooxidation under the influence of laser radiation, which is also confirmed by a change in the shape of the spectra of complex **4** in chloroform, taken before and after long-term irradiation (Figure 7).

Similar results were obtained for oil oxidation,[17] photobleaching of Eosin Y, and photochemical reaction of Cr(VI).[18,52] Previously, a change in the shape of the spectra was also observed for a dispersion of graphene oxide in water, which indicated the reduction of graphene oxide under the action of laser radiation with a wavelength of 532 nm.[36]

Research into the nature of the discovered photochemical and morphological processes of complex **4** is beyond the scope of this paper and is not considered here. Further research in this area is necessary and should be aimed at studying the stage of photochemical and morphological transformations, as well as studying the final form of *p*-chlorophenoxy substituted lutetium phthalocyanine. These studies are useful both for biomedical and pharmaceutical applications and for the development of photothermal spectroscopy in the analysis of biologically active compounds.

Conclusions

p-Chlorophenoxy substituted lutetium phthalocyanine in tetrahydrofuran and chloroform at a low concentration of 10 nmol/L was investigated using thermal lens spectrometry. A substantial change in thermal diffusivity indicates a change in the mechanism of heat release. A possible reason may be the occurrence of specific solvation and mutual influence of solvated phthalocyanine molecules, leading to structuring of the solvent. The dynamics of the thermal lens signal indicates the occurrence of photooxidation of phthalocyanine under the action of laser radiation. Photothermal methods as thermal lens spectrometry makes it possible to expand the understanding of the processes occurring in phthalocyanines and identify physicochemical changes at concentrations below 0.01 μmol/L.

Acknowledgements. This work was supported by the Russian Science Foundation (project 23-73-10076).

References

1. Cho K.T., Trukhina O., Roldán-Carmona C., Ince M., Gratia P., Grancini G., Gao P., Marszalek T., Pisula W., Reddy P.Y., Torres T., Nazeeruddin M.K. *Adv. Energy Mater.* **2016**, *7*, 1601733.
2. Urbani M., Ragoussi M.-E., Nazeeruddin M.K.,Torres T. *Coord. Chem. Rev.* **2019**, *381*, 1–64.
3. de Saja J.A., Rodriguez-Mendez M.L. *Adv. Colloid Interface Sci.* **2005**, *116*, 1–11.
4. Nikoloudakis E., Lopez-Duarte I., Charalambidis G., Ladomenou K., Ince M., Coutsolelos A.G. *Chem. Soc. Rev.* **2022**, *51*, 6965–7045.
5. Sanarova E., Meerovich I., Lantsova A., Kotova E., Shprakh Z., Polozkova A., Orlova O., Meerovich G., Borisova L., Lukyanets E., Smirnova Z., Oborotova N., Baryshnikov A. *J. Drug Deliv. Sci. Tec.* **2014**, *24*, 315–319.
6. Li X., Peng X.H., Zheng B.D., Tang J., Zhao Y., Zheng B.Y., Ke M.R., Huang J.D. *Chem. Sci.* **2018**, *9*, 2098–2104.
7. Wang W., Wang J., Hong G., Mao L., Zhu N., Liu T. *Biomacromolecules* **2021**, *22*, 4284–4294.
8. Li D., Cai S., Wang P., Cheng H., Cheng B., Zhang Y., Liu G. *Adv. Health. Mater.* **2023**, *12*, e2300263.
9. Abid S., Nguyen C., Daurat M., Durand D., Jamoussi B., Blanchard-Desce M., Gary-Bobo M., Mongin O., Paul-Roth C.O., Paul F. *Dyes Pigm.* **2022**, *197*, 109840.
10. Huber V., Sengupta S., Würthner F. *Chemistry (Weinheim an der Bergstrasse, Germany)* **2008**, *14*, 7791–7807.
11. Isago H. "Prototypical" Optical Absorption Spectra of Phthalocyanines and Their Theoretical Background. In: *Optical Spectra of Phthalocyanines and Related Compounds* (Isago H., Ed.), Springer Japan: Tokyo, **2015**. pp 21–40.
12. Bialkowski S.E., Astrath N.G.C., Proskurnin M.A. *Photothermal Spectroscopy Methods*. Wiley: **2019**. 512 p.
13. Khabibullin V.R., Usoltseva L.O., Galkina P.A., Galimova V.R., Volkov D.S., Mikheev I.V., Proskurnin M.A. *Physchem* **2023**, *3*, 156–197.
14. Proskurnin M.A., Khabibullin V.R., Usoltseva L.O., Vyrko E.A., Mikheev I.V., Volkov D.S. *Physics-Uspekhi* **2022**, *65*(3), 270–312.
15. Fomina P.S., Proskurnin M.A. *J. Appl. Phys.* **2022**, *132*, 040701.
16. Mazza G., Posnicek T., Wagner L.-M., Brandl M. *Procedia Engineer.* **2016**, *168*, 602–605.
17. Savi E.L., Malacarne L.C., Baesso M.L., Pintro P.T.M., Croge C., Shen J., Astrath N.G.C. *Spectrochim. Acta A Mol. Biomol. Spectrosc.* **2015**, *145*, 125–129.
18. Herculano L.S., Malacarne L.C., Zanuto V.S., Lukasievicz G.V., Capeloto O.A., Astrath N.G. *J. Phys. Chem. B* **2013**, *117*, 1932–1937.
19. Estupiñán-López C., Dominguez C.T., Filho P.E.C., Santos B.S., Fontes A., de Araujo R.E. *J. Lumin.* **2016**, *174*, 17–21.
20. Martins V.M., Messias D.N., Doualan J.L., Braud A., Camy P., Dantas N.O., Catunda T., Pilla V., Andrade A.A., Moncorgé R. *J. Lumin.* **2015**, *162*, 104–107.
21. Yamauchi M., Mawatari K., Hibara A., Tokeshi M., Kitamori T. *Anal. Chem.* **2006**, *78*, 2646–2650.
22. Anjos V., Andrade A.A., Bell M.J.V. *Appl. Surf. Sci.* **2008**, *255*, 698–700.
23. Proskurnin M.A.,Volkov D.S., Ryndina E.S., Nedosekin D.A., Zharov V.P. *ALT Proceedings* **2012**, *1*.
24. Mazza G., Posnicek T., Wagner L.-M., Ettenauer J., Zuser K., Gusenbauer M., Brandl M. *Sens. Actuators, B* **2017**, *249*, 731–737.
25. Soto C., Saavedra R., Toral M.I., Nacaratte F., Poza C. *Microchem. J.* **2016**, *129*, 36–40.
26. Simon J., Anugop B., Nampoori V.P.N., Kailasnath M. *Opt. Laser Technol.* **2021**, *139*, 106954.
27. Mathew R.M., Zachariah E.S., Jose J., Thomas T., John J., Titus T., Unni N.G., Mathew S., Mujeeb A., Thomas V. *Appl. Phys. A* **2020**, *126*, 828.
28. Francis F., Anila E.I., Joseph S.A. *Optik* **2020**, *219*, 165210.
29. Luna-Sánchez J.L., Jiménez-Pérez J.L., Carbajal-Valdez R., Lopez-Gamboa G., Pérez-González M., Correa-Pacheco Z.N. *Thermochim. Acta* **2019**, *678*, 178314.
30. Martelanc M., Ziberna L., Passamonti S., Franko M. *Talanta* **2016**, *154*, 92–98.
31. Deus W.B.,Ventura M., Silva J.R., Andrade L.H.C., Catunda T., Lima S.M. *Fuel* **2019**, *253*, 1090–1096.
32. Astrath N.G., Astrath F.B., Shen J., Zhou J., Michaelian K.H., Fairbridge C., Malacarne L.C., Pedreira P.R., Medina A.N., Baesso M.L. *Opt. Lett.* **2009**, *34*, 3460–3462.
33. Savi E.L., Herculano L.S., Lukasievicz G.V.B., Regatieri H.R., Torquato A.S., Malacarne L.C., Astrath N.G.C. *Fuel* **2018**, *217*, 404–408.
34. Ventura M., Deus W.B., Silva J.R., Andrade L.H.C., Catunda T., Lima S.M. *Fuel* **2018**, *212*, 309–314.
35. Proskurnin M.A., Chernysh V.V., Pakhomova S.V., Kononets M.Y., Sheshenev A.A. *Talanta* **2002**, *57*, 831–839.
36. Khabibullin V.R., Ratova D.V., Stolbov D.N., Mikheev I.V., Proskurnin M.A. *Nanomaterials (Basel)* **2023**, *13*, 2126.
37. Shen J., Lowe R.D., Snook R.D. *Chem. Phys.* **1992**, *165*, 385–396.
38. Khabibullin V.R., Usoltseva L.O., Mikheev I.V., Proskurnin M.A. *Nanomaterials (Basel)* **2023**, *13*, 1006.
39. Kuzmina E.A., Dubinina T.V., Borisova N.E., Tomilova L.G. *Macroheterocycles* **2017**, *10*, 520–525.
40. Kuzmina E.A., Dubinina T.V., Tomilova L.G. *New J. Chem.* **2019**, *43*, 9314–9327.
41. Yahya M., Nural Y., Seferoğlu Z. *Dyes Pigm.* **2022**, *198*, 109960.
42. Kuzmina E.A., Dubinina T.V., Vasilevsky P.N., Saveliev M.S., Gerasimenko A.Y., Borisova N.E., Tomilova L.G. *Dyes Pigm.* **2021**, *185*, 108871.
43. Timoumi A., Dastan D., Jamoussi B., Essalah K., Alsalmi O.H., Bouguila N., Abassi H., Chakroun R., Shi Z., Ţălu Ş. *Molecules* **2022**, *27*, 6151.
44. Zouaghi M.O., Arfaoui Y., Champagne B. *Opt. Mater.* **2021**, *120*, 111315.
45. Brennetot R., Georges J. *Spectrochim. Acta, A* **1999**, *55*, 381–395.
46. Escalona R. *Opt. Commun.* **2008**, *281*, 388–394.
47. Dovichi N.J., Bialkowski S.E. *CRC Crit. Rev. Anal. Chem.* **1987**, *17*, 357–423.
48. Netzahual-Lopantzi Á., Sánchez-Ramírez J.F., Jiménez-Pérez J.L., Cornejo-Monroy D., López-Gamboa G., Correa-Pacheco Z.N. *Appl. Phys. A* **2019**, *125*, 588.
49. Augustine A.K., Mathew S., Girijavallabhan C.P., Radhakrishnan P., Nampoori V.P.N., Kailasnath M. *J. Opt.* **2014**, *44*, 85–91.
50. Oliveira G.M., Zanuto V.S., Flizikowski G.A.S., Kimura N.M., Sampaio A.R., Novatski A., Baesso M.L., Malacarne L.C., Astrath N.G.C. *J. Mol. Liq.* **2020**, *312*, 113381.
51. Georges J. *Spectrochim. Acta A* **2008**, *69*, 1063–1072.
52. Pedreira P.R.B., Hirsch L.R., Pereira J.R.D., Medina A.N., Bento A.C., Baesso M.L., Rollemberg M.C., Franko M., Shen J. *J. Appl. Phys.* **2006**, *100*, 044906.
53. Jiménez Pérez J.L., Sanchez Ramírez J.F., Cruz Orea A., Gutiérrez Fuentes R., Cornejo-Monroy D., López-Muñoz G.A. *J. Nano Res.* **2010**, *9*, 55–60.
54. Usoltseva L.O., Volkov D.S., Avramenko N.V., Korobov M.V., Proskurnin M.A. *Nanosystems: Physics, Chemistry, Mathematics* **2018**, *9*, 17–20.
55. Fischer M., Georges J. *Spectrochim. Acta, A* **1997**, *53*, 1419–1430.
56. Lopez-Bueno C., Suarez-Rodriguez M., Amigo A., Rivadulla F. *Phys. Chem. Chem. Phys.* **2020**, *22*, 21094–21098.

57. Kawazumi H., Kaieda T., Inoue T., Ogawa T. *Chem. Phys. Lett.* **1998**, *282*, 159–163.
58. Arnaud N., Georges J. *Spectrochim. Acta, A* **2004**, *60*, 1817–1823.
59. Arnaud N., Georges J. *Spectrochim. Acta, A* **2001**, *57*, 1295–1301.
60. Zhirkov A.A., Bendrysheva S.N., Proskurnin M.A., Ragozina N.Y., Zuev B.K. *Mosc. Univer. Chem. Bull.* **2009**, *64*, 87–92.
61. Georges J., Paris T. *Anal. Chim. Acta* **1999**, *386*, 287–296.
62. Arnaud N.,Georges J. *Spectrochim. Acta, A* **2001**, *57*, 1085–1092.
63. Franko M., Tran C.D. *J. Phys. Chem.* **2002**, *95*, 6688–6696.
64. Colcombe S.M., Lowe R.D., Snook R.D. *Anal. Chim. Acta* **1997**, *356*, 277–288.
65. Zhirkov A.A., Nikiforov A.A., Tsar'kov D.S., Volkov D.S., Proskurnin M.A., Zuev B.K. *J. Analyt. Chem.* **2012**, *67*, 290–296.
66. Abbasgholi-Na B., Nokhbeh S.R., Aldaghri O.A., Ibnaouf K.H., Madkhali N., Cabrera H. *Polymers* **2022**, *14*, 2707.
67. Ruzzi V., Buzzaccaro S., Piazza R. *Polymers* **2023**, *15*, 1283.
68. Colcombe S.M., Snook R.D. *Analyt. Chim. Acta* **1999**, *390*, 155–161.
69. Khabibullin V.R., Franko M., Proskurnin M.A. *Nanomaterials (Basel)* **2023**, *13*, 430.
70. Rodriguez L.G., Iza P., Paz J.L. *J. Nonlinear Opt. Phys. Mater.* **2016**, *25*, 1650022.
71. Mohebbifar M.R. *Optik* **2021**, *242,* ,166902.
72. Leulescu M., Rotaru A., Pălărie I., Moanţă A., Cioateră N., Popescu M., Morîntale E., Bubulică M.V., Florian G., Hărăbor A., Rotaru P. *J. Therm. Anal. Calorim.* **2018**, *134*, 209–231.
73. Dubinina T.V., Paramonova K.V., Trashin S.A., Borisova N.E., Tomilova L.G., Zefirov N.S. *Dalton Trans.* **2014**, *43*, 2799–2809.
74. Rauf M.A., Hisaindee S., Graham J.P., Nawaz M. *J. Mol. Liq.* **2012**, *168*, 102–109.
75. Lebedeva N.S., Petrova O.V., Vyugin A.I., Maizlish V.E., Shaposhnikov G.P. *Thermochim. Acta* **2004**, *417*, 127–132.
76. Slota R., Dyrda G. *Inorg. Chem.* **2003**, *42*, 5743–5750.
77. Voronina A.A., Filippova A.A., Znoiko S.A., Vashurin A.S., Maizlish V.E. *Russ. J. Inorg. Chem.* **2015**, *60*, 1407–1414.
78. Vashurin A., Filippova A., Znoyko S., Voronina A., Lefedova O., Kuzmin I., Maizlish V., Koifman O. *J. Porphyrins Phthalocyanines* **2015**, *19*, 983–996.
79. Kurian A., Bindhu C.V., Nampoori V.P.N. *J. Opt.* **2015**, *37*, 43–50.

Received 16.04.2024
Accepted 08.07.2024